Electronic Supplementary Material (ESI) for Environmental Science: Nano.

Supplementary data

Protonation of Rhodanine Polymers for Enhancing Capture and Recovery of Ag^+ from Highly Acidic Wastewater

Xiaocui Yin[a,b], Penghui Shao[a], Lin Ding[a], Yu Xi[a], Kai Zhang[a], Liming Yang[a], Hui Shi[a], and Xubiao Luo*[,a,b]

[a] Key Laboratory of Jiangxi Province for Persistent Pollutant Control and Resource Recycling

Nanchang Hangkong University, Nanchang, 330063, P. R. China

E-mail: luoxubiao@126.com

[b] College of Chemistry, Nanchang University, Nanchang, 330063, P. R. China

Text Sections: S1 – S3

Figures: S1 – S9

Table: S1-S2

S1 Adsorption isotherms

Adsorption equilibrium experiments were carried out to examine the adsorption capacity of PAR for Ag^+ ions with the initial concentration range of 10-1200 mg L^{-1} at pH −0.2. According to **Fig. S4**, the adsorption capacities for Ag^+ ions increased with increasing Ag^+ concentration, and the maximum adsorption amount or monolayer coverage was achieved at the initial concentration of 800 mg L^{-1}. The Langmuir and Freundlich models were used to fit the adsorption data. The linearized Langmuir and Freundlich isotherms can be described as following equations:

Langmuir model: $$\frac{C_e}{Q_e} = \frac{C_e}{Q_m} + \frac{1}{k_l \bullet Q_m} \qquad \text{(s1)}$$

Freundlich model: $$\lg Q_e = \frac{1}{n}\lg C_e + \lg k_f \qquad \text{(s2)}$$

Where C_e (mg L^{-1}) and Q_e (mg g^{-1}) are, respectively, the concentration and adsorbed amount of Ag^+ at adsorption equilibrium. K_l and K_f represent the Langmuir constant (L g^{-1}) and the Freundlich constant ($mg^{1-(1/n)}$ $L^{1/n}$ g^{-1}), respectively; Q_m is the maximum adsorption capacity (mg g^{-1}) of the adsorbent. The corresponding fitting results were listed in **Table S2**.

The sorption isotherms fit Langmuir model better than Freundlich model due to the larger correlation coefficient (R^2), suggesting that Ag^+ sorption on PAR is monolayer sorption process.

S2 Adsorption kinetics

The adsorption kinetics of Ag^+ adsorption on polymer were investigated, and the results were described in **Fig. S6**. In addition, the polymer demonstrated good performances in the first 50 min and then reach the equilibrium after 100 min.

To discern the rate-controlling step in the adsorption process of Ag^+ ions, rate constants of adsorptions were analyzed by the pseudo-first-order and pseudo-second-order kinetic models, respectively, which can be expressed as:

$$\ln(q_e - q_t) = \ln q_e - k_1 t \qquad (3)$$

$$\frac{t}{q_t} = \frac{1}{k_2 q_e^2} + \frac{t}{q_e} \qquad (4)$$

where t represents the contact time (min); q_t and q_e denotes the amount of Ag^+ adsorbed at a given time t and at equilibrium (mg g^{-1}), respectively. k_1 (min^{-1}) and k_2 (g mg^{-1} min^{-1}) are the rate constants of adsorption, respectively.

Plots of the experimental data and the model fitting were illustrated in **Fig.S6**. The correlation kinetic parameters from both models were listed in **Table S1**. From the correlation coefficients (R^2) data, we think that the adsorption process of Ag^+ ions are more suitable for the pseudo-second-order kinetic model. In addition, the theoretical *qe* values calculated by the pseudo-second order model were 239.2 mg g^{-1}, which is closer to experiments value 235.0 mg g^{-1}. Apparently, the adsorption behavior for Ag^+ ion is more consistent with the pseudo-second-order kinetics model, suggesting that the adsorption rate is controlled by the chemical adsorption.

S3 Dubinin-Radushkevich (D-R) model

The linearized D-R model is expressed as the following equation:

$$\ln q_e = \ln q_m - K_{DR}\varepsilon^2 \tag{2}$$

where q_e and q_m are the disequilibrium and theoretical saturation capacity, respectively; K_{DR} denotes the constant which is related to the mean free energy of adsorption; ε is the Polanyi potential which can be calculated by using the following formula:

$$\varepsilon^2 = RT\ln(1+\frac{1}{C_\mathrm{e}}) \tag{3}$$

where parameters R, T and Ce denote the ideal gas constant, the adsorption temperature in Kelvin (K) and the equilibrium concentration, respectively. q_m and K_{DR} could be calculated from the intercept and slope of the plot for lnq_e against ε^2. Subsequently, the adsorption energy (E) can be obtained by the following equation:

$$E = (2K_{DR})^{-1/2} \tag{s4}$$

The relationship between adsorption energy and adsorption processes can be well demonstrated by the adsorption energy which was calculated from the above formula. when E is less than 8 kJ mol^{-1}, the physical adsorption dominates the reaction; when E is between 8 to 16 kJ mol^{-1}, the ion-exchange dominates the reaction; when E is between 20 to 40 kJ mol^{-1}, chemical adsorption dominates the reaction.

Figures

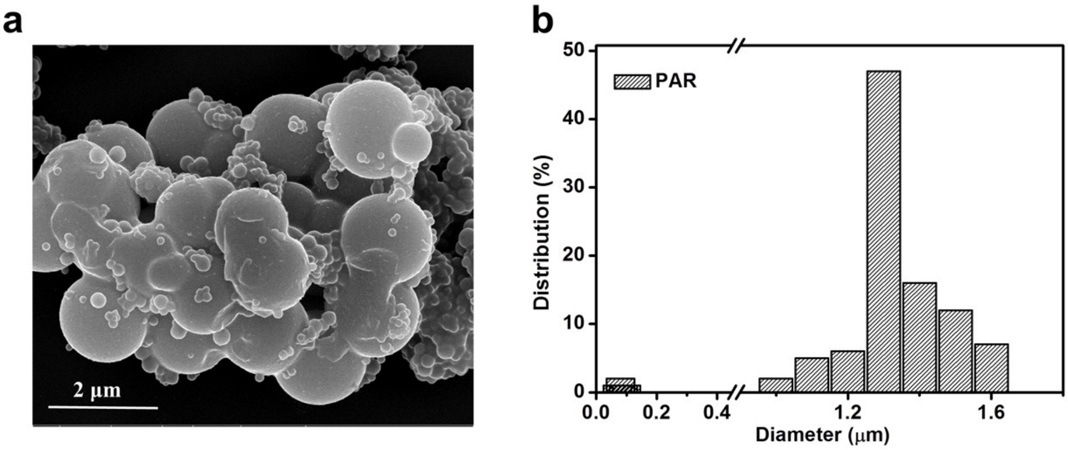

Fig. S1 (a) SEM image of PAR and (b) particle size distribution mapping.

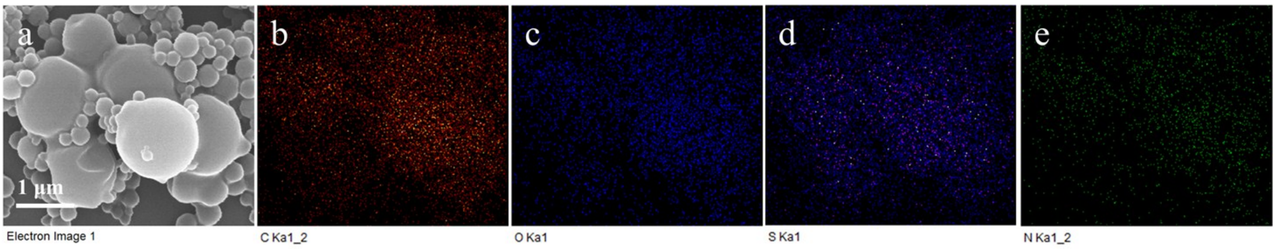

Fig. S2 (a) SEM image and the corresponding EDS mappings for (b) C, (c), O, (d) S, (e) N elements of PAR before adsorption Ag^+.

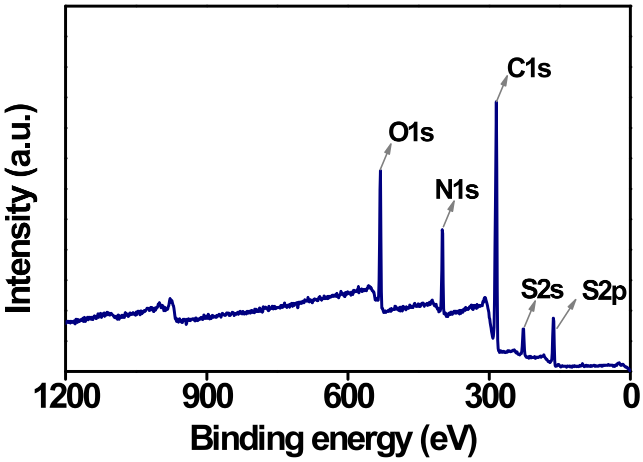

Fig. S3 XPS full-scan spectrum of PAR

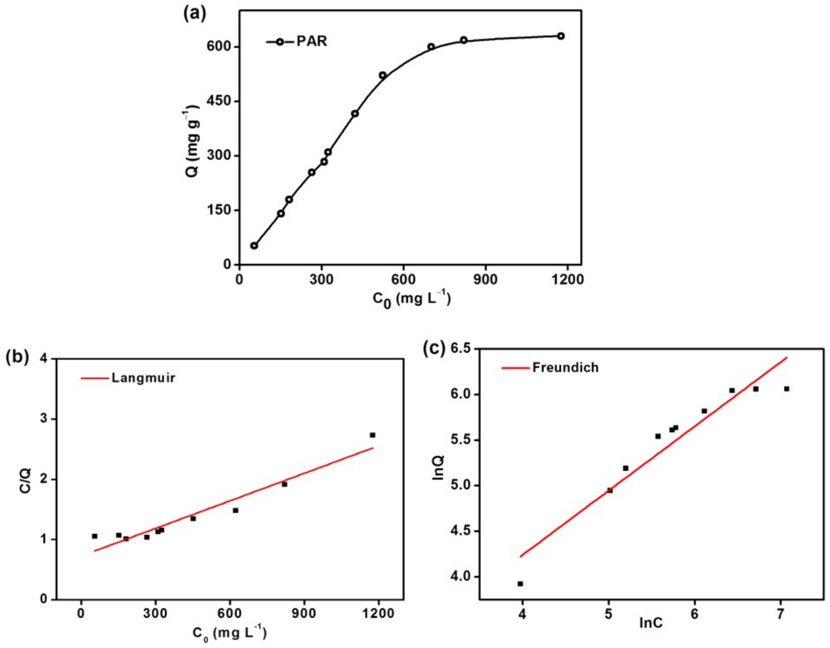

Fig. S4 (a) Effects of Ag^+ initial concentration on the adsorptivity of PAR; The corresponding fitting results by the (b) Langmuir model and (c) Freundlich model.

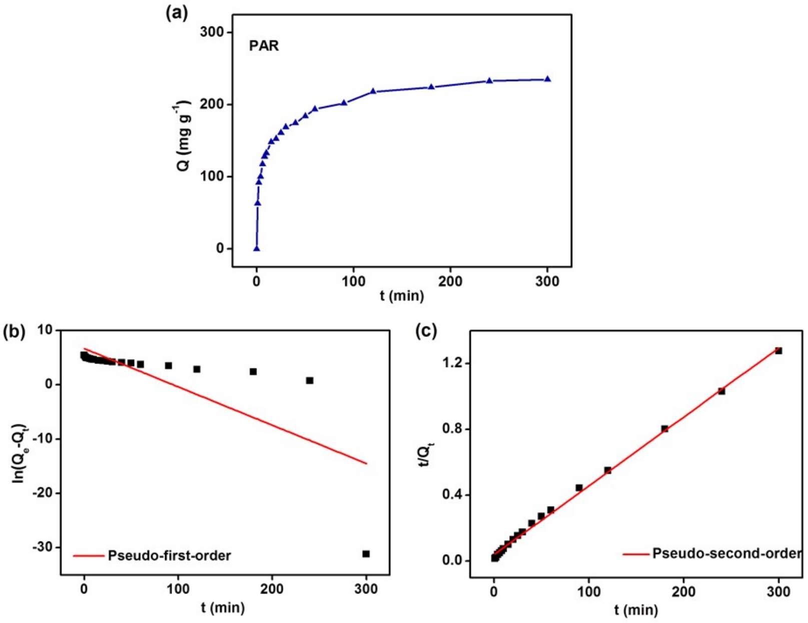

Fig. S5 (a)Effect of equilibrium time on the adsorption of Ag^+ by PAR. (b) Pseudo-first-order and (c) Pseudo-second-order kinetic for Ag^+ adsorption by PAR.

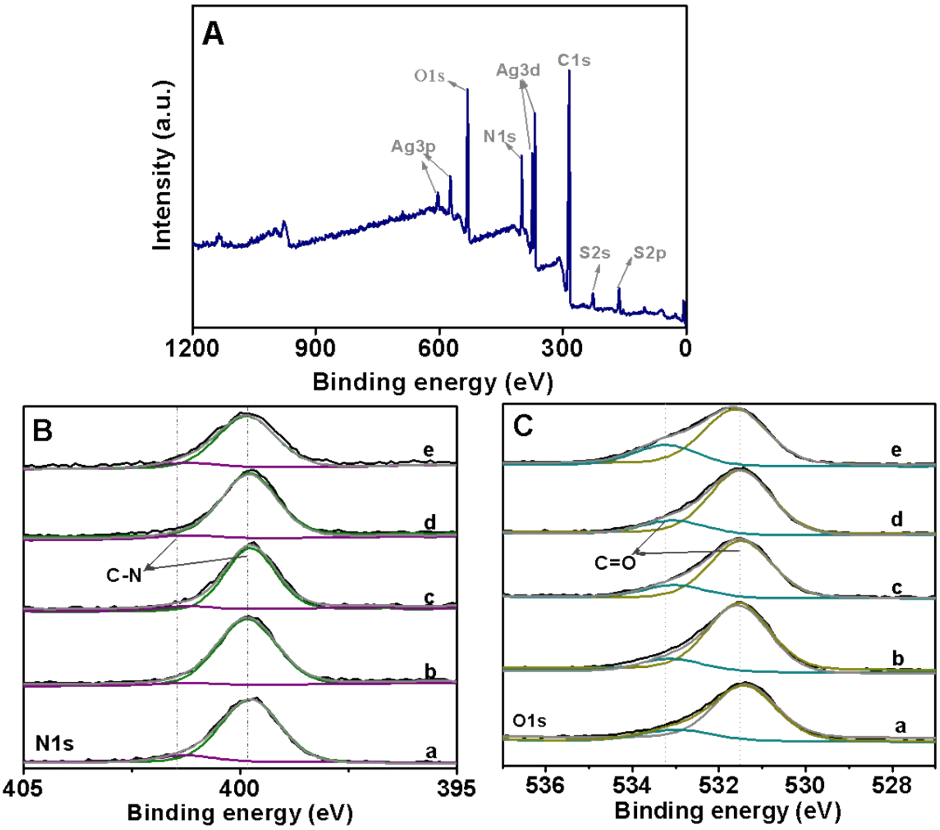

Fig. S6 XPS full-scan spectrum of PAR after adsorption of siliver (A); High-resolution XPS spectra of N1s (B) and O1s (C) for the PAR before (a) and after adsorption of silver under different pH (b-e: pH=2.0, 1.0, 0.0, −0.2)

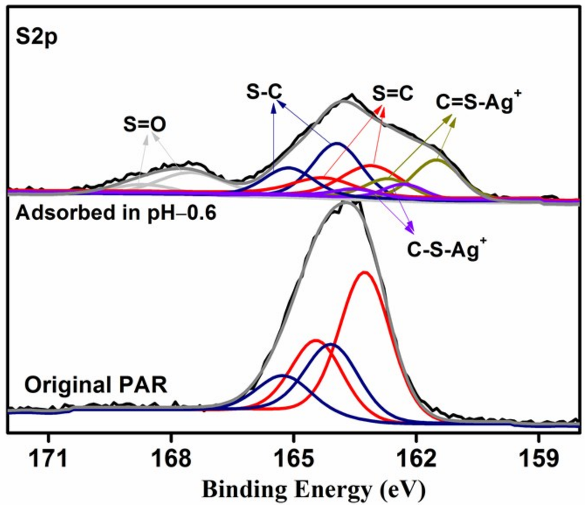

Fig. S7 The high resolution XPS spectra of S2p of polyallylrhodanine and after adsorption at pH= −0.6

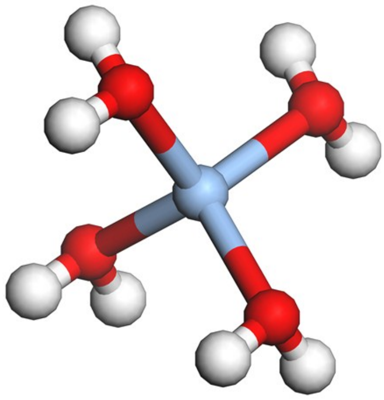

Fig. S8 The structure of hydrated Ag$^+$ ion. The colour of atom: white: H; red: O; cyan: Ag).

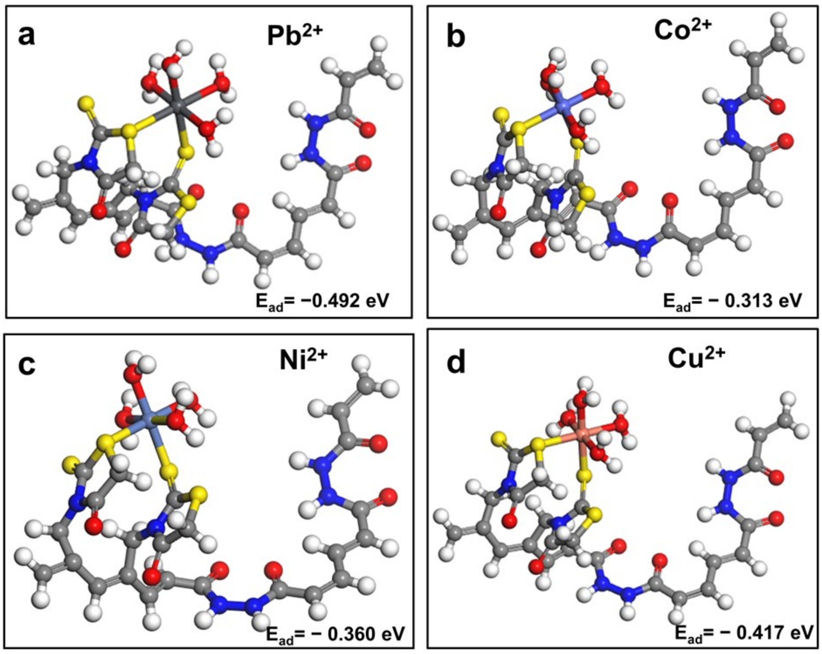

Fig. S9 Adsorption energies (E_{ad}) of PAR combined with various metal ions. (a) Pb^{2+}, (b) Co^{2+}, (c) Ni^{2+}, (d) Cu^{2+}.

Tables

Table S1. Fitting results by the Langmuir and Freundlich models.

Langmuir constants			**Freundlich constants**		
Q_m (mg g^{-1})	**k_l (L mg^{-1})**	**R^2**	**k_f ($mg^{1-(1/n)}$ $L^{1/n}$ g^{-1})**	**n**	**R^2**
653	0.0021	0.9227	26.27	1.417	0.9094

Table S2 Adsorption kinetic parameters of PAR.

	K	**Q_{cal} (mg g^{-1})**	**R^2**
Pseudo-first order	7.051×10^{-2} min^{-1}	778	0.5410
Pseudo-second order	4.368×10^{-4} g mg^{-1} min^{-1}	239	0.9976